Manuscript Title

Multi-Scale Modeling of Intensive Macroalgae Cultivation and Marine Nitrogen Sequestration

Meiron Zollmann[a]*, Boris Rubinsky[b], Alexander Liberzon[c] and Alexander Golberg[a].

[a]Porter School of Environmental and Earth Sciences, Tel Aviv University, Israel; and [b]Department of Mechanical Engineering, University of California at Berkeley, CA, US; and [c]School of Mechanical Engineering, Tel Aviv University, Israel.

*Corresponding author: Meiron Zollmann

Email: meironz@mail.tau.ac.il

Keywords

Nearshore Cultivation; Biosequestration; Estuarine Bioremediation; Biorefinery Feedstock; Ulva;

Abstract

Multi-scale macroalgae growth models are required for the efficient design of sustainable, economically viable and environmentally safe farms. Here, we develop a multi-scale model for Ulva sp. macroalgae growth and nitrogen sequestration in an intensive cultivation farm, regulated by temperature, light and nutrients. The model incorporates a range of scales by incorporating spatial effects in two steps: light extinction at the reactor scale (1 m) and nutrient absorption at the farm scale (1 km). The model was validated on real data from an experimental reactor installed in the sea. Biomass production rates, chemical compositions and nitrogen removal were simulated under different seasons, levels of dilution in the environment and water-exchange rate in the reactor. This multi-scale model provides an important tool for environmental authorities and seaweed farmers who desire to upscale to large bioremediation and/or macroalgae biomass production farms, thus promoting the marine sustainable development and the macroalgae-based bioeconomy.

Introduction

Marine conservation and sustainable development is essential for achieving the United Nations' Sustainable Development Goals[1]. Large scale seaweed farms (> 1 km) could proffer a sustainable and environmentally safe means for biomass production for biorefineries, to supply the soaring demand for food, energy and raw materials, without expanding agricultural lands or freshwater requirements[2–5]. Furthermore, seaweed aquaculture can be utilized for eutrophication mitigation[6–9], thus contributing to the international effort to abate nutrient over-enrichment in coastal ecosystems[10,11] (i.e. the Mediterranean Action Plan [5]). However, the implementation of commercial cultivation of seaweed beyond East Asia countries is limited, because of a lack of farming tradition, undeveloped markets, and a questionable economic viability[12]. Large-scale commercial macroalgae cultivation, which is considered a new technology in most countries, could be advanced using multi-scale models. The use of multi-scale models to promote new technologies in reduced time and cost was demonstrated in the Carbon Capture Simulation Initiative (CCSI)[13]. The CCSI, a partnership among national laboratories, industry, and universities, was established to enable accelerated commercialization of carbon capture technologies by developing multiscale models and simulation tools, used to improve design and

reduce scale-up risk. Similarly, advances in cultivations of seaweed from small-scale activities to large scale implementation could also benefit from the availability of multiple scale models. We propose that these multi-scale models could facilitate the design and optimization of large seaweed farms by incorporating in the large scale models data from cultivation activities in a small scale[14,15], and demonstrate it in a study with mathematical and experimental parts.

Current macroalgae growth and nutrient dynamics models were developed for specific applications. For example, long-term ecological models that attempt to predict macroalgal productivity and seasonal blooms in prone ecosystems[16,17,26,27,18–25] or "black box" culture models that focus mostly on on-shore photobioreactors or tanks[9,28] or offshore extensive cultivation[29–31]. These models, which pursue a basic understanding of the thermodynamics of individual algae thalli and photobioreactors[32], can provide a general idea about productivity and seasonal effects on algae growth. However, they do not incorporate spatial effects at the scale of the farm and its environment and therefore cannot predict how the algae would behave in a real-life large-scale farm. On the other hand, as proposed above, multi-scale models that extend from the scale of a single plant to the scale of the farm could be used for the design of real-life scale seaweed farms[15]. Such a multi-scale model could incorporate available small-scale mathematical models and small-scale experimental data. This challenging task involves the combination of multiple biological, engineering and environmental factors and is the focus of this research.

Recently, some studies have proposed to apply intensified macroalgae cultivation, usually done in photobioreactors, also at near- and off-shore seaweed farms[33,34]. Intensified cultivation systems rely on frequent harvesting and could benefit from temporal multi-scale models that can predict biomass production and chemical composition in a time scale of days. As a case study, we used data from a Mediterranean Sea near-shore intensive growth experimental reactor used for free-floating *Ulva* species cultivation, which was described by Chemodanov et al.[34]. This reactor employs airlift pumps and bottom aeration and is suitable for shallow coastal areas or estuarine systems, in which macroalgae have a natural important role in nutrient cycling[22]. As these environments are the most prone to harmful eutrophication[35,36] which is responsible for significant environmental and economic damages[36], the added value of nutrient bio-sequestration may increase the economic viability of seaweed cultivation in such locations.

In this study we develop a theoretical multi-scale model for macroalgae growth and nitrogen sequestration in an intensive cultivation seaweed farm, which is regulated by temperature, light and nutrients **(Fig. 1)**. The model is used to simulate farm-scale biomass production and nitrogen removal in a nutrient-enriched environment, at a temporal and spatial resolution and scale that is not available today. Specifically, the model predicts farmed seaweed biomass and sequestered N in different seasons. The model incorporates the required nutrient concentrations and how is the spatial distribution of biomass composition and productivity affected by levels of airlift pumping and dilution in the environment. Our model enables the investigation of farm spatial and temporal responses to environmental variations and provides useful insights on the effects of farm design and operation on the compliance with environmental and commercial requirements (i.e uniform biomass composition and minimal energy consumption). Altogether, this multi-scale model provides an important tool for environmental authorities and seaweed farmers who desire to upscale to large bioremediation and/or macroalgae biomass production farms, thus promoting the macroalgae-based bioeconomy.

Results and Discussion

Calibrated model. The calibration process started with light extinction parameters (K_a and K_0) and continued to growth function parameters (parameters of eq 1 and SI appendix, eq S1). Based on a scan of 600 parametric combinations within a pre-defined range, which was built based on literature values (SI appendix, Table S2), we manually fitted parametric combinations that provide

both good RMSREs (<15%) and experiment-specific good relative errors (<20%). We used both criteria to prevent over- or under dominance of specific returns and environmental conditions (i.e three returns with a low error and one with a high error). The chosen parametric combination yielded $RMSRE_1 = 10.3\%$ for the first step and $RMSRE_2 = 13.7\%$ for the second step (SI appendix, **Figs. S5-8** and Table S3).

Light extinction parameters. We found that the model is not sensitive to K_0 in the examined range as the optical path in water is short. The best fit between in- and ex-situ light intensity measurements were found using a light extinction coefficient of K_a= 0.15 (SI appendix, **Fig. S10**), which is higher than the previously used K_a = 0.01[9] for *Ulva*, but similar to values used for other algae species[37]. The higher value better represents the significant effect of biomass density on light extinction.

Growth function parameters. f_{Temp} parameters, T_{opt} and T_{max}, were adjusted to 18 and 31.5℃, fitting the literature optimal temperature range of 15-20℃[38,39]. K_I was adjusted to 20 µmol photons $m^{-2}{\cdot}s^{-1}$ (SI appendix, **Fig. S11**). However, K_I is a flexible parameter and is known to decrease when the *Ulva* is acclimated to low light intensities[40]. λ_{20} was adjusted to 2.2% day^{-1} (0.16% light $hour^{-1}$, SI appendix, **Fig. S11**), which is low compared to literature values (5-6.5% day^{-1}). A limitation of this study is that the calibration system was mostly P-limited (N:P >20 [2]), a fact that is not represented in the model and may lead to underestimations of biomass production under P-saturation conditions. Furthermore, the agreement between modelled and measured final N_{int} was low, which may be a result of the P-limitation, as high N:P ratio can inhibit N uptake[39].

Sensitivity analysis. The parameter with the largest total effect on the total biomass production and N bio-sequestration (Sobol sensitivity index of 0.35-0.4 in the range of 0 to 1) is K_a. K_I and λ_{20}, with total sensitivity indexes of 0.15-0.28 and 0.09-0.1, respectively, have a moderate effect, and μ_{max} has a weak effect (~0.02) on total biomass production and N bio-sequestration. N_{env}, in comparison, is highly sensitive only to *d* (sensitivity index of 0.97). The effect of other parameters within examined range is negligible (<0.01) (**Fig. 2**). This analysis shows that our multi-scale model is sensitive to parameters related to light (f_I), which, in the simulated climate, limits growth only in winter when days are short and sky may be cloudy, and when biomass density in reactor is high. The sensitivity of the model to parameters related to N ($\psi_{N_{ext}}$ and $f_{N_{int}}$), on the other hand, is low, as both reach a steady state relatively rapidly in N rich environments and affect model outcomes only when N_{ext} and N_{int} are low (i.e N_{ext} below K_S or N_{int} below $N_{\mathrm{int\ crit}}$). The low sensitivity to N related parameters can be understood in greater depth by the time-scale separation idea[41]. In diluting environments (*d* > 0), small changes in *d* have significant effects on the results of the multi-scale model as they force rapid N_{env} and N_{ext} attenuation regardless of biomass uptake. contrarily, small changes in Q_P have no effect on model results as throughout the examined range N supply does not limit growth. The model was found to be insensitive to f_{Temp} and f_S related parameters in the simulated environmental conditions, but this finding should be examined with a wider range of temperatures and salinities. Model sensitivity to λ_{20} was higher than the sensitivity to μ_{max} probably due to the dependence of µ also on other parameters (T, S, I and N_{int}), that lessen the direct effect of μ_{max} on model results.

Seasonal trends in biomass production and nitrogen removal. Productivity and N sequestration vary significantly seasonally, ranging between 0 and 26.8 $gDW{\cdot}day^{-1}{\cdot}m^{-2}$ (0-30 $gDW{\cdot}day^{-1}{\cdot}m^{-3}$) and between 0.2 and 1.2 $gN{\cdot}day^{-1}{\cdot}m^{-2}$ (0.2-1.3 $gN{\cdot}day^{-1}{\cdot}m^{-3}$), with average values of 13.3 $gDW{\cdot}day^{-1}{\cdot}m^{-2}$ (14.9 $gDW{\cdot}day^{-1}{\cdot}m^{-3}$) and 0.7 $gN{\cdot}day^{-1}{\cdot}m^{-2}$ (0.8 $gN{\cdot}day^{-1}{\cdot}m^{-3}$) (**Fig. 3**). In a farm of 100 chained reactors (cultivation area of 200 m^2), this translates into annual productivity of 1210 $gC{\cdot}m^{-2}{\cdot}year^{-1}$, almost four times the estimated average productivity of terrestrial biomass in the Middle East (290 $gC{\cdot}m^{-2}{\cdot}year^{-1}$[,42]) and N sequestration of 249 $gN{\cdot}m^{-2}$ $year^{-1}$. Peak production is expected from the end of February till the middle of March, and a second production peak is found in November. Production during the summer is very low, which is explained by high water temperatures (SI appendix, **Fig. S12**). Therefore, effective bio-sequestration cannot be

applied during the summer in the modeled conditions. The apparent differences in N sequestration between the diluting environment (d>0), in which high and low N_{env} water is mixed, and the non-diluting environment (d=0) is discussed below in the spatial effects section.

To reduce environmental N levels below a defined, environmentally benign, level, different seasons require different sizes of the seaweed farm. Considering that a 10 μM threshold prevents extreme eutrophication[43], to avoid damage to the environment, in winter, the dimension of the farm should be 1,462 m^2, in spring the farm should be 914 m^2 and in the fall 1,192 m^2 (**Fig. 4a**). From the perspective of the model, these dimensions of the farm are between 600 to 900 reactor size macro elements, i.e. the assumption that the single element control volume used in the analysis is small relative to the entire domain of analysis is acceptable. As important, these results demonstrate the value of this analysis. They provide a measure on how to design a large seaweed farm that is safe for the environment.

Following are additional examples of how this multi-scale model can be used to design large seaweed farms. A farm designed according to winter N sequestration abilities will produce 7.1 tons DW·year^{-1}, whereas farms designed according to spring or autumn sequestration abilities will produce only 4.4 or 5.8 tons DW·year^{-1}, respectively. As a general trend, in high N_{env} levels, the relationship between added reactors and N sequestration is linear, but in lower N levels, closer to K_S, uptake is slower, and more reactors are needed per sequestration unit. **Figs. 4b-d** present N and biomass dynamics in the last reactor in a farm designed to achieve the threshold in all seasons (731 reactors). Fixed year-round cultivation cycles result in time and space non-uniform chemical composition. However, uniform chemical composition can be achieved by adjusting lengths of cultivation cycles to environmental conditions, specifically, temperature, day length and N_{env}. Shortening autumn and spring cultivation cycles to 11 and nine days, respectively, for example, will enable the production of biomass with constant N_{int}, although won't comply with the defined 10 μM threshold during the spring (SI appendix, **Fig. S13**). However, shorter cultivation cycles come at an expense of higher labor demand and do not necessarily grant higher accumulated yields.

Spatial effects controlled by dilution and pumping. In our model, spatial effects on biomass composition and growth rate appear only when N_{env} decreases to limiting levels. The rate of this decrease can be controlled by airlift pumping flow and is accelerated in a diluting environment.

Pumping flow. Q_p can be manipulated to control N flux into reactors and thus also chemical composition and growth rate of the algae (**Fig. 5**). The immediate effect of Q_p is on the N_{env} vs N_{ext} dynamics. High Q_p minimizes differences between N_{env} and N_{ext}, which leads to a faster reduction in N_{env}[1] and slower reduction in N_{ext}[2] compared to the trajectories of N_{env} and N_{ext} with lower Q_p[3,4]. Simulating reactors without pumps ($Q_p = 0$, dark blue line) decouples N_{ext} from N_{env} and eliminates the spatial effects of nutrient absorption. Thus, although N_{env} does not change, rapid depletion of N_{ext} leads to a decrease in N_{int} which is followed by a decrease in produced biomass. Therefore, in the described system pumping is essential. High Q_p promotes bio-sequestration but may result in a steeper spatial gradient of N_{int}[5] compared to low Q_p[6]. Finally, Q_p can be manipulated according to farm design requirements, controlling farm size and biomass composition. It should be mentioned that water exchange by pumping has additional important contributions, such as the supply of inorganic carbon, removal of waste material which may inhibit growth, and temperature control[34,44]. Furthermore, in an estuarine environment, pumping water from 1-2 m below the surface can increase salinity, which is crucial for the growth of marine macroalgae species. However, water pumping is an energy-consuming component of seaweed farms and should be optimized to minimize its carbon footprint. Previous trials to cultivate *Ulva* in the described reactors without water exchange were unsuccessful in our group[34]. However, a thorough review of seaweed cultivation[44] mentioned that water exchange in *Ulva* cultivation can

be reduced to 10% day^{-1}, equivalent to 15 l·hour^{-1} in our work, without a significant change in yield.

Dilution. In highly diluting environments, bio-sequestration would be usually ineffective. However, such environments are not prone to eutrophication and do not require nutrient removal. **Fig. 6** presents the spring system dynamics in a 100-reactors farm, subjected to 5% dilution between each two reactors, similar to dilution rates used in literature[30]. Compared to the first reactor (darkest green), which is not affected by dilution, downstream reactors meet lower N_{env} concentrations which are translated into lower N_{ext} and gradually into lower N_{int} and lower biomass production. In the simulated conditions (N_{env_0} = 500μM), annual decrease in biomass production due to dilution (968 to 962 kgDW, 0.6%) is significantly smaller than the annual decrease in N sequestration (50 to 32 kgDW, 36%) (**Fig. 3**). This difference can be explained by the production of low protein biomass in the downstream, diluted, areas. Larger farms may not be practical in high-dilution locations, as downstream N_{env} concentrations would not allow any growth beyond what the initial N_{int} allows. However, using high-protein upstream biomass as a continuous seeding feedstock for further cultivation may enable sustainable low protein biomass production in such an environment. Following a similar concept, previous works suggested performing a two-step cultivation process, starting with high biomass production in a nutrient-rich environment and finishing with carbohydrate accumulation in nutrient-limited environment[45]. As opposed to the protein-rich biomass that is produced in N enriched environments and can be used for food and feed applications, such carbohydrate-rich biomass is advantageous for the extraction of different polysaccharides (i.e starch, ulvan and cellulose) and can be processed into various forms of biofuels and chemicals[4].

A few previous studies assessed the effectiveness of eutrophication bioremediation in China by macroalgae cultivation. Generally, this was examined by comparing N and P open sea levels in cultivation season and off-season, by calculating how much nutrients were removed based on published data and biomass composition analysis, and by following eutrophication symptoms, such as hypoxia and harmful algal blooms[7,46,47]. One study, by Fan et al.[6], advanced into actively increasing nutrient removal by ecological engineering, specifically artificial upwelling, which is the pumping of nutrient-rich deep water to the surface. Fan et al.[6] found that artificial upwelling can increase the average yield of kelp seaweed by 55 g per plant, and developed a few useful recommendations regarding the conditions in which intensified cultivation can be worthwhile. Although in a different setup and framework, our work strengthens their recommendation to optimize pump operation according to algae requirements (nutrients, water exchange and salinity and temperature control), environmental conditions and regulations, and energy costs. These considerations change seasonally and spatially, even within the farm itself. Our model, developed especially for this cause, can help relating to spatial differences during the design and the operation of seaweed farms.

The environmental significance of this work relates to two major environmental issues: climate change and water pollution. The model developed in this work can be used to quantify and optimize the environmental significance of large-scale seaweed farms, specifically eutrophication mitigation. Thus, bioremediation by seaweed farms can be advanced from an unplanned external benefit to an inherent part of coastal development. Furthermore, if eutrophication mitigation is compensated by the authorities, this model can play a key role and incentivize the establishment of new seaweed farms, accompanied by additional environmental and economic benefits, on the local (i.e. marine conservation and economic development) and global (i.e. carbon sequestration, sustainable biomass supply and mitigation of fresh water stress) scales. In addition, with some modifications, this model can be used to model fish cages and integrated multi-trophic aquaculture (IMTA) and promote sustainable aquaculture and marine development.

Conclusions

We developed a multi-scale model for *Ulva* sp. macroalgae growth and nitrogen sequestration in an intensive cultivation farm, regulated by temperature, light and nutrients. The model enables spatial simulations by incorporating light extinction effects at the reactor scale (1 m) and nutrient absorption effects at the farm scale (1 km). Specifically, we simulated: 1. year-round productivities and N sequestration in the farm; 2. the farm size required for eutrophication mitigation in different seasons; and 3. spatial distribution of biomass production, chemical composition and environmental N along the farm in different dilution rates in the environment and in different airlift pumping flows.

The high-resolution spatial and temporal model developed in this work, is an important step toward implementing precision agriculture techniques in seaweed aquaculture. Such advanced techniques are expected to improve productivities, efficiencies and accompanied environmental benefits, leading the way to sustainable marine development, accompanied by multiple economic and environmental benefits regarding climate change and water pollution mitigation.

Future studies need to validate the model on higher-resolution data of all state variables and engage in uncertainty quantification in different scales. In general, the robustness of the model will increase by further calibrating it with wider and more diverse empiric data sets, that will raise additional important constraining factors. Future efforts to improve the model should include adjusting it to P limited environments and relating to various phenomena that cause uncertainty in macroalgae cultivation. These phenomena include, for example, an unexplained decline in biomass, sudden sporulation, age, and history effect on the growth rate, water flow effects on growth and chemical composition and pest damage. By improving the ability to understand and describe both temporal and spatial phenomena in a seaweed farm in a resolution of days, these improved models should help to optimize the design of seaweed farms to combine environmental improvement and commercial viability.

Materials and Methods

Our model incorporates multi-scale spatial effects: light extinction at the reactor scale and nutrient absorption at the farm scale, into a mathematical model of the *Ulva* sp. macroalgae metabolism [2] (See schematic description in **Fig. 1**). The spatial effects employ the following multiscale procedures: 1. from a single thallus scale (1 cm) to a reactor scale (1 m), relating to light extinction in the reactor, and 2. from a reactor scale to a farm-scale (1 km), relating to nutrient absorption in the farm.

The model was calibrated using experimental data from the reactor scale and qualified with a sensitivity analysis. Thereafter, biomass production rates, chemical compositions and farm-scale nitrogen removal was simulated under different seasons, levels of dilution in the environment (0-5% dilution ratio between every two reactors) and water-exchange rate in the reactor (0, 15 and 460 l·hour^{-1}). The entire code of this project is available as an open source in https://doi.org/10.5281/zenodo.4062432.

Model assumptions. The *Ulva* metabolic model assumes that the dynamics of the limiting nutrient, in this case nitrogen (N), under the constraining effects of environmental conditions (light intensity (I), temperature (T) and salinity (S)) predicates the dynamics of biomass growth and chemical composition. In the marine environment, the limiting nutrient is usually N[48] and our model focuses on N limited environments. However, similar models can be developed also for other elements such as phosphorus (P) and ferrous that may limit growth too in some marine environments. Our model also assumes that the organic carbon reserve, depending on carbon uptake and photosynthesis rates, is not limiting within the modelled conditions. The model follows the Droop Equation concept, in which the effect of the external, environmental, nutrient concentration on growth is mediated by internal nutrient concentrations ("cell quota")[16,49]. This is

rather important as changes in internal N concentration occur gradually in a typical time scale of days whereas significant changes in environmental N concentrations may occur much faster, on a time scale of hours[50].

Our multi-scale model relates to cultivation in semi-closed reactors with controlled water exchange. This leads to the differentiation between nutrient concentrations inside the reactor that interact with the biomass directly, named here external N, and nutrient concentrations outside the reactor that are affected only secondarily named here environmental N. Environmental N is the connecting agent that passes onwards in the flow the accumulating signal of changing N concentrations, which is translated into spatial differences in biomass composition and growth rate.

We used as a reference a cultivation reactor (cage) described by Chemodanov et al.[34]. Each reactor is assumed to be well-mixed by bottom aeration and is connected to an airlift pump that supplies the reactor with fresh seawater and nutrients. We also assume water flow through reactor boundaries is negligible.

We simulate the large-scale farm as composed of a continuum of macroscopic reactor size elements (compartments). This type of mass transfer model is commonly used in pharmaceutics which studies mass transfer through macroscopic units referred to as compartment[51]. The model assumes that the conditions in each reactor size control volume (compartment) can be accurately represented by one average value (external N) and that the domain of analysis (farm) is much larger than the macroscopic reactor size element.

We define our large-scale farm model as a 3D model (SI appendix, **Fig. S1**). The x-axis is the direction of the flow and all simulations relate to one row of reactors in this direction. Each reactor constitutes an N sink, causing the spatial change of environmental N concentrations in the direction of the flow (x). By assuming the width of this change is small concerning the distance between the rows, this model becomes applicable also to multiple rows of reactors, with no variation in the y-axis. Finally, although light extinction increases with depth, potential variations in biomass with depth (z-axis) can be averaged out due to the well-mixed reactors' assumption.

Model Governing Equations. The multi-scale model is based on four governing ordinary differential equations (ODEs), describing the mass balance of four state variables: biomass density in a reactor (m, g Dry Weight (DW)·l^{-1}, eq 1), biomass internal concentration of N ($\boldsymbol{N_{int}}, \%\ \mathbf{gN \cdot gDW^{-1}}, \mathbf{eq\ 2}$), external concentration of N in the reactor ($\boldsymbol{N_{ext}},\ \boldsymbol{\mu mol - N \cdot l^{-1}}, \mathbf{eq\ 3}$) and the environmental N concentration outside the reactor ($\boldsymbol{N_{env}},\ \boldsymbol{\mu mol - N \cdot l^{-1}}, \mathbf{eq\ 4}$) under varying temperatures, light intensities and salinities.

$$\frac{\partial m}{\partial t} = (\mu - \lambda)m, \qquad (1)$$
$$\mu = \mu_{max} f_{Temp} f_S \min\{f_{N_{int}}, f_{P_{int}}, f_I\}$$
$$\text{Initial Condition (I.C):}\ m_{(x,t=0)} = m_0$$

Where μ (h^{-1}) is biomass specific growth rate formulated of μ_{max} (h^{-1}), the maximum specific growth rate, and f_{Temp}, f_S, $f_{N_{int}}$, $f_{P_{int}}$ and f_I, which are the T, S, N_{int},, P_{int}, and I growth functions[2] (see more in SI). λ is biomass specific losses rate as a function of T and is formulated of λ_{20} (h^{-1}), the specific rate of biomass losses and θ, an empiric factor of biomass losses[2]. λ does not include losses by grazing, sporulation and fragmentation by storms, which vary between different environments and are highly affected by extreme events. We adjusted daily specific growth and losses rates to hourly rates, assuming for simplicity that growth and biomass losses occur only during light hours (see details in SI). This assumption ignores night growth that occurs due to metabolites produced during light-time photosynthesis[52], and thus distorts growth distribution throughout the day. However, the assumption does not affect total daily growth and therefore does not impair the model accuracy at a temporal resolution of days to weeks.

$$\frac{\partial N_{int}}{\partial t} = \psi_{N_{ext}} - N_{\text{int}}\mu m \qquad (2)$$
$$\psi_{N_{ext}} = \frac{N_{\text{intmax}} - N_{\text{int}}}{N_{\text{intmax}} - N_{\text{intmin}}} \frac{V_{\max} N_{\text{ext}}}{K_S + N_{\text{ext}}}$$
$$\text{I.C: } N_{\text{int}\ (x,t=0)} = N_{\text{int}\ 0}$$

Where $\psi_{N_{ext}}$ (μmol-N·gDW^{-1}·h^{-1}) is the N uptake function, formulated of N_{intmax} and N_{intmin} (% gN · gDW^{-1}), the maximum and minimum N_{int} concentrations, respectively, V_{max} (μmol-N·gDW^{-1}·h^{-1}), the maximum N uptake rate and K_S (μmol-N·l^{-1}), the N half-saturation uptake constant. $-N_{\text{int}}\mu m$ describes N_{int} dilution in biomass by growth.

$$\frac{\partial N_{ext}}{\partial t} = \frac{Q_p(N_{env} - N_{ext})}{V_{cage}} - \psi_{N_{ext}} m \qquad (3)$$
$$\text{I.C: } N_{\text{ext}\ (x,t=0)} = N_{\text{ext}_0}$$

Where Q_{p} (l·h^{-1}) is the airlift pumping flow and V_{cage} (m^3) is the reactor volume. The change in N_{ext} is the sum of N in incoming airlift pump flow, N in reactor overflow and N uptake by the biomass in the reactor.

$$\frac{\partial N_{env}}{\partial t} = \frac{\left[-Q_s\left(N_{env_{x-1}}(1-d) - N_{env_x}\right) - Q_p\left(N_{env_x} - N_{ext_x}\right)\right]}{V_{cage}} \qquad (4)$$
$$\text{I.C: } N_{\text{env}_{(x,t=0)}} = N_{\text{ext}_0}\text{, Boundary Condition (B.C): } N_{\text{env}_{(x=0,t)}} = N_{\text{ext}_0}$$

Where N_{env_x} is N_{env} below reactor x at time t, $N_{env_{x-1}}$ is N_{env} below reactor x-1 at time t, d (%) is the dilution ratio between every two reactors and Q_s (l·h^{-1}) is the stream flow through an area equivalent to the reactor narrow-side cross-section. Thus, the change in N_{env} is the sum of incoming N flows (upstream flow and reactor overflow) and outflowing flows (downstream flow and airlift pumping into the reactor). All four ODEs were solved numerically with hourly time steps.

Scale Elements in Model. The multi-scale model has two scale elements:1. light extinction at the reactor scale that requires dynamic averaging of light intensity per biomass unit, and 2. nutrient absorption at the farm scale that requires following the dynamics of environmental N.

Single Thallus to Reactor. In the metabolic model of a single thallus scale, growth is affected directly by incident light intensity (eq 5). In transition to a reactor scale, light intensity is averaged per biomass unit, as formulated by Oca et al.[9] (eq 6). This formulation considers water depth in the reactor, biomass density and light extinction coefficients of both water and biomass. In both equations, we multiplied I_0 by a 0.43 PAR constant, representing the ratio of the sunlight which is suitable for photosynthesis[53].

$$f(I) = \frac{I}{K_I + I}\, PAR \qquad (5)$$

Where I and K_I (μmol photons·m^{-2}·s^{-1}) are incident light intensity and light half-saturation constant, respectively.

$$f(I) = \frac{I_{average}}{K_I + I_{average}} PAR \qquad (6)$$

$$I_{average} = \frac{I_0}{K_0 Z + K_a SD}\left[1 - \exp\left(-(K_0 Z + K_a SD)\right)\right]$$

Where $I_{average}$ and I_0 (μmol photons·m^{-2}·s^{-1}) are average photon irradiance in the reactor and incident photon irradiance at water surface, respectively, SD (gDW·m^{-2}) is stocking density of biomass per unit of water surface in the reactor, K_0 (m^{-1}) is water light extinction coefficient, Z (m) is maximum water depth in the reactor and K_a (m^2·gDW^{-1}) is *Ulva* light extinction coefficient.

Reactor to Farm. In a single well-mixed reactor, nutrient reduction by biomass is local and does not accumulate along the stream. Therefore, eq 4, describing changes in N_{env}, is redundant. However, in a seaweed farm, spatial variations in N_{env} cannot be described without eq 4 that connects the reactors and the environment. Eq 3, describing changes in N_{ext}, was derived from the Convection–Diffusion equation[54] (eq 7). Eq 4, describing changes in N_{env}, is based on the same equation, without the uptake term.

$$\frac{\partial N_{ext}}{\partial t} = \nabla \cdot (D \nabla N_{ext}) - \nabla \cdot (\mathrm{v} N_{ext}) - \psi_{N_{ext}} m \quad (7)$$

Where D ($m^2 \cdot s^{-1}$) is the average diffusivity coefficient of dissolved inorganic N species and v ($m \cdot s^{-1}$) is the velocity field in which the dissolved nitrogen is moving. Both eq 3 and eq 4 are derived from this equation, with specific simplifying assumptions: 1. D constant in space; 2. incompressible velocity flow, and 3. zero net diffusivity, as the reactor is well-mixed and there is no concentration gradient ($\nabla N_{ext} = 0$). Therefore, N_{ext} in the reactor is affected only by the N supply by airlift pump (normalized to reactor volume) and N uptake by algae. Eq 4, describing changes in N_{env}, follows the same principal form but without the uptake term.

Model Calibration. We calibrated the model parameters using experimental growth data of *Ulva* cultivation in a single well-mixed sea-based reactor from Chemodanov et al.[34] (SI appendix, **Figs. S3-4** and Table S1). Model was calibrated by manipulating model parameters and minimizing two types of root mean square relative errors (RMSRE): 1. RMSRE between biomass growth projected values (PV) based on in-situ I measurements compared to biomass growth PV based on ex-situ measurements, and 2. RMSRE between ex-situ I based PV and experimentally measured growth values. See full description of calibration process in SI appendix.

Sensitivity analysis. To examine how each parameter, in a defined range (SI appendix, Table S2), influences model simulations output, we analyzed farm-scale sensitivity of state variables using SALib, the Sensitivity Analysis Library in Python[55]. Specifically, the analysis focused on the projected values of total produced biomass, total accumulated N_{int} and average final N_{env}, under the simulation frame of a 100-reactors' farm and one cultivation period per season, that should suffice to observe both temporal and spatial effects of the different parameters. First, 10 values and 420 random parametric combinations of all model parameters (SI appendix, Table S2) were generated using the Saltelli method[56,57]. Next, each combination was run through the model, producing an array of possible biomass production, N accumulation and final N_{env} results. Finally, the results were analyzed using the Sobol analysis[58], giving each parameter a first order and total sensitivity index between zero and one.

Model Simulations. The model was applied to simulate year-round cultivation of *Ulva* sp. in a row of cultivation reactors in a nutrient-enriched estuary environment located in a semi-arid climate. Data regarding nutrient concentrations, salinities, water temperature and flow was taken from the long-term study of Suari et al.[59] on the Alexander estuary, located in the center of Israel (SI appendix, **Fig. S12** and Table S4). I data was extracted from the IMS database from the Israel Meteorological Services (https://ims.data.gov.il/he/ims/6). Although S varies with depth and can change dramatically according to flesh flood events and formation of sandbar breaches[59], effect on growth was minor and we used a constant value of S=30 PSU. All constraining environmental factors except nutrients were assumed to be constant in space. Each cultivation cycle started with a constant set of initial conditions ($m_0, N_{int,0}, N_{ext,0}$ and $N_{env,0}$) which applied to all reactors. Harvesting back to initial biomass was performed every two weeks, and accumulated biomass production was calculated. In addition, N removal from the environment was calculated as the difference between total N in final and initial biomass. Specific simulations of seasonal N removal capacity were used to project the number of reactors needed to achieve a 10 μM-N level threshold, which is below levels found in extremely eutrophicated zones[43], in each season. Finally, a spatial perspective was added by examining the system dynamics under various

pumping levels and in a diluting environment, in which the enriched N_{env} water is diluted by mixing with lower N_{env} water (i.e. 5% dilution between each two reactors).

Acknowledgments

The authors thank the TAU-Berkeley fund for funding and Tzachi Yaffe for assistance in the graphic design of figures.

Contributions

Meiron Zollmann has designed and performed the research, analyzed the data and wrote the paper. Boris Rubinsky, Alexander Liberzon and Alexander Golberg have designed and performed the research, contributed analytic tools and wrote the paper.

Ethics declarations

The authors declare no competing interests.

References

1. Thomsen, M. & Zhang, X. Life cycle assessment of macroalgal ecoindustrial systems. in *Sustainable Seaweed Technologies. Cultivation, Biorefinery, and Applications* (Elsevier, 2020).
2. Lehahn, Y., Ingle, K. N. & Golberg, A. Global potential of offshore and shallow waters macroalgal biorefineries to provide for food, chemicals and energy: feasibility and sustainability. *Algal Res.* **17**, 150–160 (2016).
3. Fernand, F. *et al.* Offshore macroalgae biomass for bioenergy production: Environmental aspects, technological achievements and challenges. *Renew. Sustain. Energy Rev.* (2016). doi:http://dx.doi.org/10.1016/j.rser.2016.10.046
4. Zollmann, M. *et al.* Green technology in green macroalgal biorefineries. *Phycologia* **58**, (2019).
5. Desa, U. N. *TRANSFORMING OUR WORLD: THE 2030 AGENDA FOR SUSTAINABLE DEVELOPMENT UNITED NATIONS UNITED NATIONS TRANSFORMING OUR WORLD: THE 2030 AGENDA FOR SUSTAINABLE DEVELOPMENT*. (2016).
6. Fan, W. *et al.* Nutrient Removal from Chinese Coastal Waters by Large-Scale Seaweed Aquaculture Using Artificial Upwelling. *Water* **11**, 1754 (2019).
7. Xiao, X. *et al.* Nutrient removal from Chinese coastal waters by large-scale seaweed aquaculture. *Nat. Publ. Gr.* (2017). doi:10.1038/srep46613
8. Rose, J. M. *et al.* Nutrient Bioextraction. *Encycl. Sustain. Sci. Technol.* (2015). doi:10.1007/978-1-4939-2493-6_944-1
9. Oca, J., Cremades, J., Jiménez, P., Pintado, J. & Masaló, I. Culture of the seaweed Ulva ohnoi integrated in a Solea senegalensis recirculating system: influence of light and biomass stocking density on macroalgae productivity. *J. Appl. Phycol.* **31**, 2461–2467 (2019).
10. Kanter, D. R., Chodos, O., Nordland, O., Rutigliano, M. & Winiwarter, W. Gaps and opportunities in nitrogen pollution policies around the world. *Nat. Sustain.* 1–8 (2020). doi:10.1038/s41893-020-0577-7
11. Boesch, D. F. *Challenges and Opportunities for Science in Reducing Nutrient Over-enrichment of Coastal Ecosystems*. **25**, (2002).
12. Radulovich, R. *et al.* Farming of seaweeds. *Seaweed Sustain.* 27–59 (2015). doi:10.1016/B978-0-12-418697-2.00003-9
13. Miller, D. C. *et al.* Carbon Capture Simulation Initiative: A Case Study in Multiscale Modeling and New Challenges. *Annu. Rev. Chem. Biomol. Eng.* **5**, 301–323 (2014).

14. Wood, D., Capuzzo, E., Kirby, D., Mooney-McAuley, K. & Kerrison, P. UK macroalgae aquaculture: What are the key environmental and licensing considerations? *Mar. Policy* **83**, 29–39 (2017).
15. Van Der Molen, J. *et al.* Modelling potential production and environmental effects of macroalgae farms in UK and Dutch coastal waters. *biogeosciences Discuss.* (2017). doi:10.5194/bg-2017-195
16. Martins, I. & Marques, J. C. A Model for the Growth of Opportunistic Macroalgae (Enteromorpha sp.) in Tidal Estuaries. *Estuar. Coast. Shelf Sci.* **55**, 247–257 (2002).
17. Port, M. A. (Alex). Measuring and modelling estuarine macroalgae blooms and water column nutrients. (2016).
18. Martins, I. *et al.* Significant variations in the productivity of green macroalgae in a mesotidal estuary: Implications to the nutrient loading of the system and the adjacent coastal area. *Mar. Pollut. Bull.* **54**, 678–690 (2007).
19. Port, A., Bryan, K. R., Pilditch, C. A., Hamilton, D. P. & Bischof, K. Algebraic equilibrium solution of tissue nitrogen quota in algae and the discrepancy between calibrated parameters and physiological properties. *Ecol. Modell.* **312**, 281–291 (2015).
20. Nixon, S. W. & Brush, M. J. Modeling the role of macroalgae in a shallow sub-estuary of Narragansett Bay, RI (USA). *Ecol. Modell.* **221**, 1065–1079 (2010).
21. Aldridge, J. N. & Trimmer, M. Modelling the distribution and growth of 'problem' green seaweed in the Medway estuary, UK. in *Eutrophication in Coastal Ecosystems* 107–122 (Springer Netherlands, 2009). doi:10.1007/978-90-481-3385-7_10
22. Lavaud, R., Filgueira, R., Nadeau, A., Steeves, L. & Guyondet, T. A Dynamic Energy Budget model for the macroalga Ulva lactuca. *Ecol. Modell.* **418**, 108922 (2020).
23. Duarte, P. & Ferreira, J. G. A model for the simulation of macroalgal population dynamics and productivity. *Ecol. Modell.* **98**,
24. Seip, K. L. A computational model for growth a n d harvesting of the marine alga ascophyllum nodosum. *Ecol. Model.* **8**, 189–199 (1980).
25. Aveytua-Alcázar, L., Camacho-Ibar, V. F., Souza, A. J., Allen, J. I. & Torres, R. Modelling Zostera marina and Ulva spp. in a coastal lagoon. *Ecol. Modell.* **218**, 354–366 (2008).
26. Solidoro, C., Pecenik, G., Pastres, R., Franco, D. & Dejak, C. Modelling macroalgae (Ulva rigida) in the venice lagoon: Model structure identification and first parameters estimation. *Ecol. Modell.* **94**, 191–206 (1997).
27. Ren, J. S., Barr, N. G., Scheuer, K., Schiel, D. R. & Zeldis, J. A dynamic growth model of macroalgae: Application in an estuary recovering from treated wastewater and earthquake-driven eutrophication. *Estuar. Coast. Shelf Sci.* **148**, 59–69 (2014).
28. Friedlander, M., Galai, N. & Farbstein, H. *A model of seaweed growth in an outdoor culture in Israel*. *Hydrobiologia* **204**, (1990).
29. Broch, O. J., Slagstad, D., Broch, O. J. & Slagstad, · D. Modelling seasonal growth and composition of the kelp Saccharina latissima. *J Appl Phycol* **24**, 759–776 (2012).
30. Petrell', R. J., Tabrizi, K. M., Harrison, P. J. & Druehl, L. D. *Mathematical model of Laminaria production near a British Columbian salmon sea cage farm*. *Journal of Applied Phycology* **5**, (1993).
31. Hadley, S., Wild-Allen, K., Johnson, C. & Macleod, C. Modeling macroalgae growth and nutrient dynamics for integrated multi-trophic aquaculture. *J. Appl. Phycol.* **27**, 901–916 (2015).
32. Zollmann, M., Traugott, H., Chemodanov, A., Liberzon, A. & Golberg, A. Exergy efficiency of solar energy conversion to biomass of green macroalgae Ulva (Chlorophyta) in the photobioreactor. *Energy Convers. Manag.* **167**, (2018).
33. Golberg, A. & Liberzon, A. Modeling of smart mixing regimes to improve marine biorefinery productivity and energy efficiency. *Algal Res.* **11**, 28–32 (2015).
34. Chemodanov, A. *et al.* Feasibility study of *Ulva* sp. (Chlorophyta) intensive cultivation in a coastal area of the Eastern Mediterranean Sea. *Biofuels, Bioprod. Biorefining* **13**, 864–877 (2019).
35. McCrackin, M. L., Jones, H. P., Jones, P. C. & Moreno-Mateos, D. Recovery of lakes and

coastal marine ecosystems from eutrophication: A global meta-analysis. *Limnol. Oceanogr.* **62**, 507–518 (2017).

36. Gren, I. M. & Limburg, K. Nutrient Recycling and Waste Treatment as a Service from Estuarine and Coastal Ecosystems. in *Treatise on Estuarine and Coastal Science* **12**, 181–198 (Elsevier Inc., 2012).
37. Béchet, Q., Shilton, A. & Guieysse, B. Modeling the effects of light and temperature on algae growth: State of the art and critical assessment for productivity prediction during outdoor cultivation. *Biotechnology Advances* **31**, 1648–1663 (2013).
38. Steffensen, D. A. The effect of nutrient enrichment and temperature on the growth in culture of Ulva lactuca L. *Aquat. Bot.* **2**, 337–351 (1976).
39. Fan, X. *et al.* The effect of nutrient concentrations, nutrient ratios and temperature on photosynthesis and nutrient uptake by Ulva prolifera: Implications for the explosion in green tides. *J. Appl. Phycol.* **26**, 537–544 (2014).
40. Sand-Jensen', K. *Photosynthetic responses of Ulva lactuca at very low light*. *int-res.com* **50**, (1988).
41. Gunawardena, J. Time-scale separation – Michaelis and Menten's old idea, still bearing fruit. *FEBS J.* (2013).
42. Monfreda, C., Ramankutty, N., & Foley, J. A. Farming the planet: 2. Geographic distribution of crop areas, yields, physiological types, and net primary production in the year 2000. *Global Biogeochem. Cycles* **22(1)**, (2008).
43. Boynton, W. R., Murray, L., Hagy, J. D., Stokes, C. & Kemp, W. M. A comparative analysis of eutrophication patterns in a temperate coastal lagoon. *Estuaries* **19**, 408–421 (1996).
44. Friedlander, M. Israeli R & D activities in seaweed cultivation. *Isr. J. Plant Sci.* **56**, 15–28 (2008).
45. Korzen, L., Pulidindi, I. N., Israel, A., Abelson, A. & Gedanken, A. Marine integrated culture of carbohydrate rich Ulva rigida for enhanced production of bioethanol. *RSC Adv.* **5**, 59251–59256 (2015).
46. Wu, H. *et al.* Bioremediation efficiency of the largest scale artificial Porphyra yezoensis cultivation in the open sea in China. *Mar. Pollut. Bull.* **95**, 289–296 (2015).
47. He, P. *et al.* Bioremediation efficiency in the removal of dissolved inorganic nutrients by the red seaweed, Porphyra yezoensis, cultivated in the open sea. *Water Res.* **42**, 1281–1289 (2008).
48. Zollmann, M., Traugott, H., Chemodanov, A., Liberzon, A. & Golberg, A. Deep Water Nutrient Supply for an Offshore Ulva sp. Cultivation Project in the Eastern Mediterranean Sea: Experimental Simulation and Modeling. *Bioenergy Res.* **12**, 1113–1126 (2019).
49. Lemesle, V. & Mailleret, L. A Mechanistic Investigation of the Algae Growth "Droop" Model. *Acta Biotheor.* **56**, 87–102 (2008).
50. Pérez-Mayorga, D. M. *et al.* Nitrogen uptake and growth by the opportunistic macroalga Ulva lactuca (Linnaeus) during the internal tide. *J. Exp. Mar. Bio. Ecol.* **406**, 108–115 (2011).
51. Rubinsky, B. The Energy Equation for Freezing of Biological Tissue. *J. Heat Transfer* **111**, 988–997 (1989).
52. Fort, A. *et al.* Extensive variations in diurnal growth patterns and metabolism among ulva spp. Strains. *Plant Physiol.* **180**, 109–123 (2019).
53. Mottus, M., Sulev, M., Baret, F., Reinart, A. & Lopez, R. Photosynthetically Active Radiation : Measurement and Modeling. (2011).
54. Thomas, S. *Introduction to Climate Modelling*. (Springer Science & Business Media, 2011).
55. Herman, J. & Usher, W. SALib: An open-source Python library for Sensitivity Analysis. *J. Open Source Softw.* **2**, 97 (2017).
56. Saltelli, A. Making best use of model evaluations to compute sensitivity indices. *Comput. Phys. Commun.* **145**, 280–297 (2002).
57. Saltelli, A. *et al.* Variance based sensitivity analysis of model output. Design and estimator

for the total sensitivity index. *Comput. Phys. Commun.* **181**, 259–270 (2010).

58. Sobol, I. M. Global sensitivity indices for nonlinear mathematical models and their Monte Carlo estimates. *Math. Comput. Simul.* **55**, 271–280 (2001).

59. Suari, Y. *et al.* Sandbar Breaches Control of the Biogeochemistry of a Micro-Estuary RIME-restoration of Israeli micro estuaries View project Effect of water circulation on the Yarqon River ecosystem View project. *Front. Mar. Sci.* (2019). doi:10.3389/fmars.2019.00224

574 **Figures**

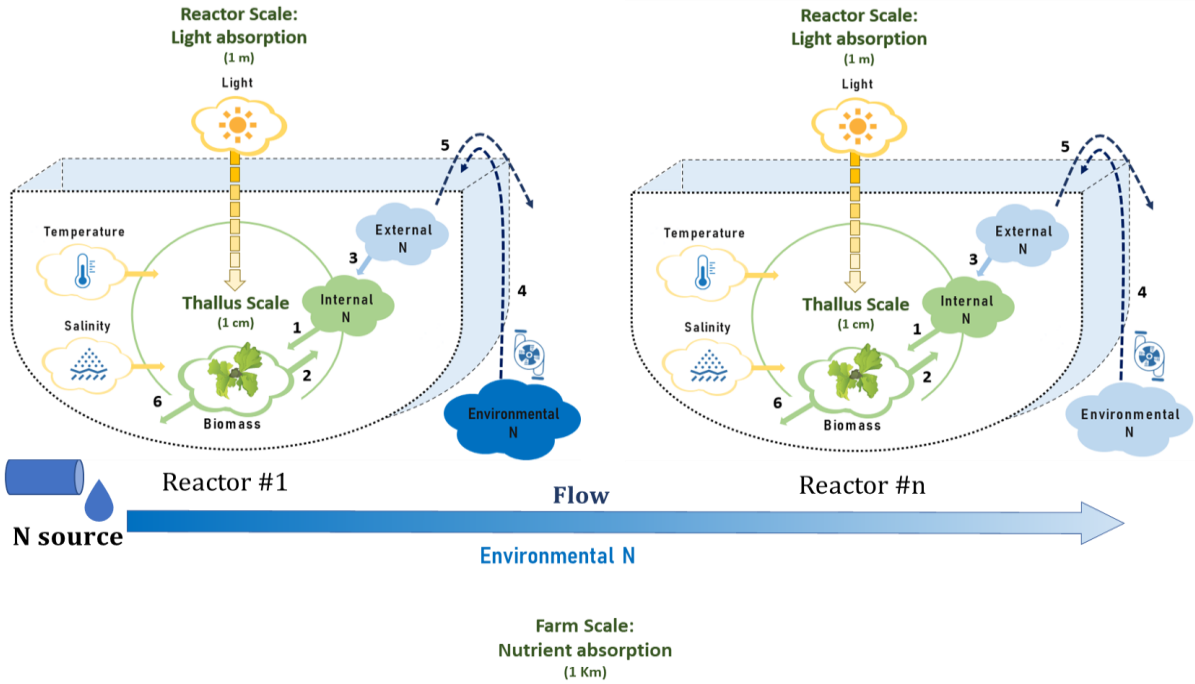

575

576 **Fig. 1.** A schematic description of the multi-scale model. The thallus scale (1 cm, green circle) is
577 composed of a simple metabolic model of Ulva, in which the production of new biomass (Ulva
578 icon) is affected by internal nitrogen (N, full green cloud) and by constraining environmental
579 conditions, including light intensity, salinity and temperature (yellow clouds). The reactor scale (1
580 m, U shape pictures) adds light extinction effects (yellow graduated arrow), the concentration of
581 external N in the reactor and the concentration of environmental N outside the reactor (dark/light
582 blue clouds, depending on N concentration). The farm-scale (1 km, row of reactors starting at
583 Reactor #1 and counting downstream to Reactor #n) adds the nutrient reduction caused by
584 absorption in reactors along with the flow (Blue graduated arrow). Green and blue clouds
585 represent the model state variables. Numbers represent the following processes: 1. Biomass
586 growth; 2. Dilution of internal N by growth; 3. N uptake; 4-5. Water exchange by airlift pumping
587 and overflow, and 6. Biomass losses.

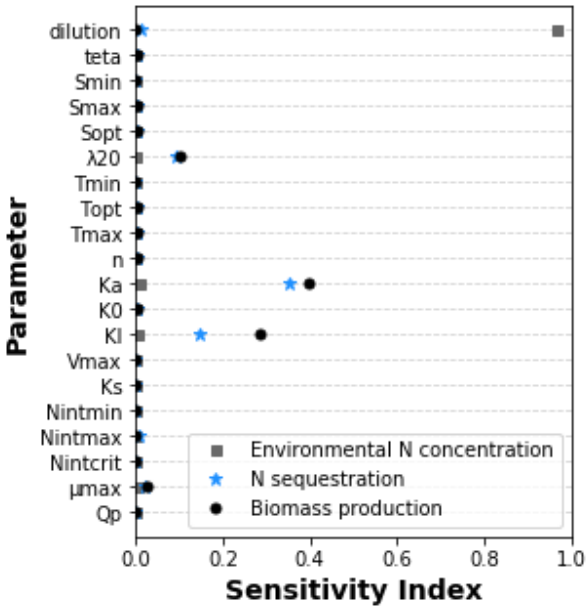

588 **Fig. 2.** Illustrated sensitivity of simulated biomass production (black circles), N sequestration (blue
589 stars) and final environmental N levels (grey squares) to model parameters, as measured by the
590 Sobol method.

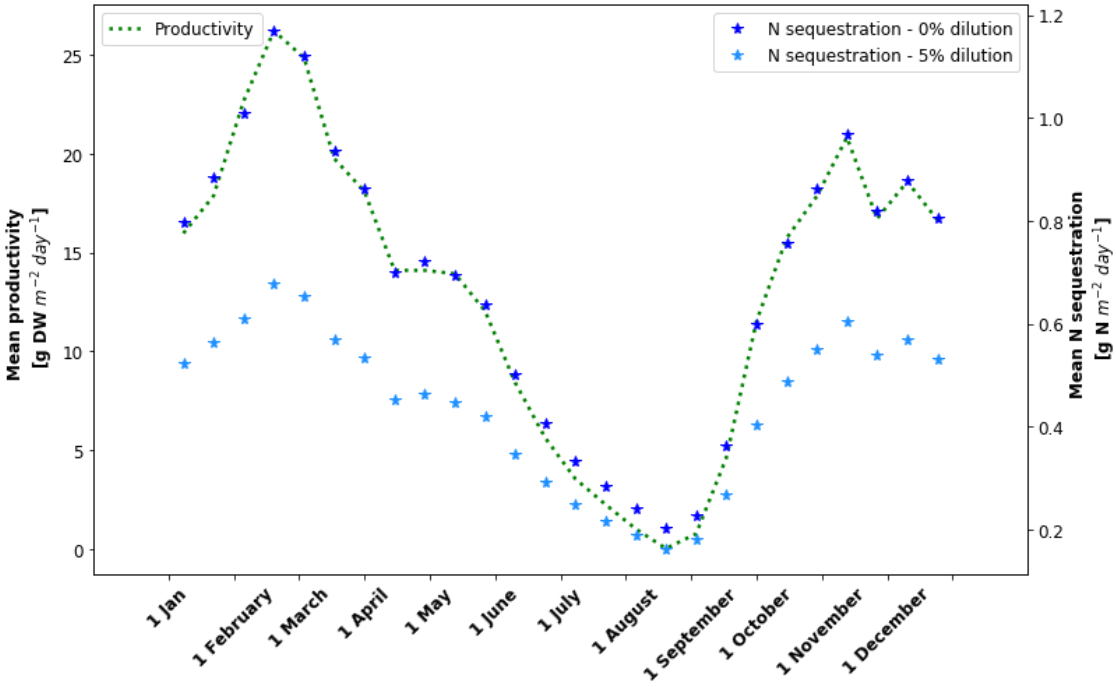

Fig. 3. Mean productivity (gDW·m^{-2}·day^{-1}, green dashed line) and mean nitrogen sequestration (gN·m^{-2}·day^{-1}) in a non-diluting environment (*d* =0, dark blue stars) and a diluting environment (*d* =0.05, 5% dilution between each two reactors, light blue stars) vs week of the year for a farm of 100 reactors.

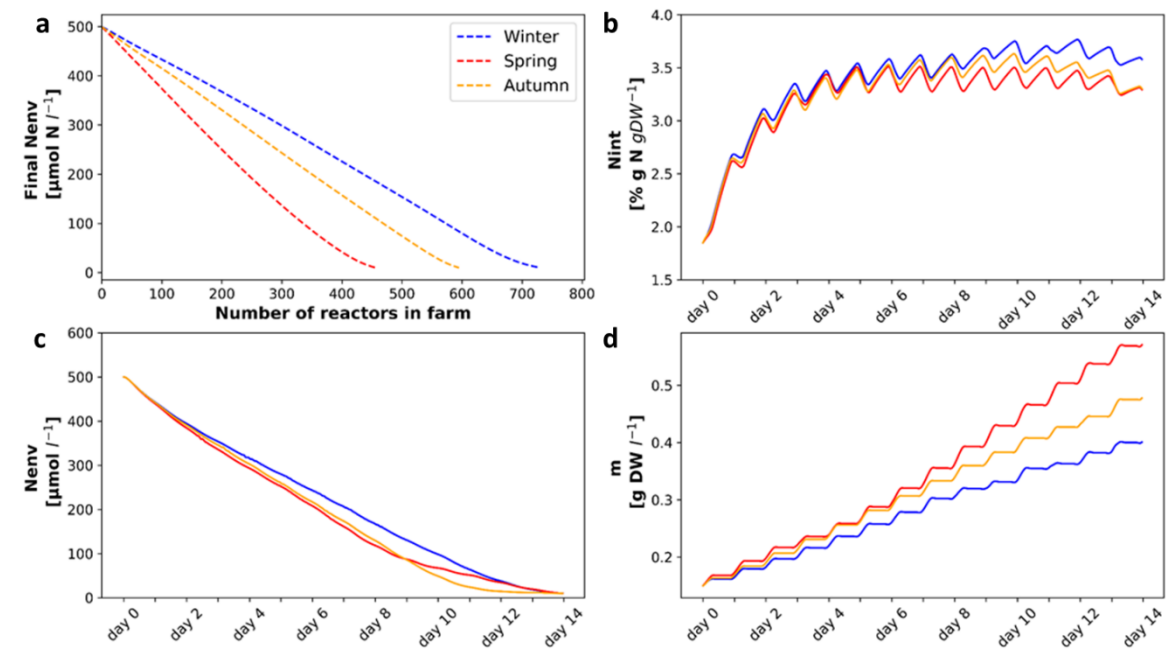

Fig. 4. (a) Final N_{env} concentration (µM-N) as a function of the number of reactors in different seasons (Winter in blue, Spring in red and Autumn in yellow)**, (b-d)** N_{env}, N_{int} and m dynamics along 14 days' cultivation periods in different seasons, for the last reactor in a farm of 731 reactors.

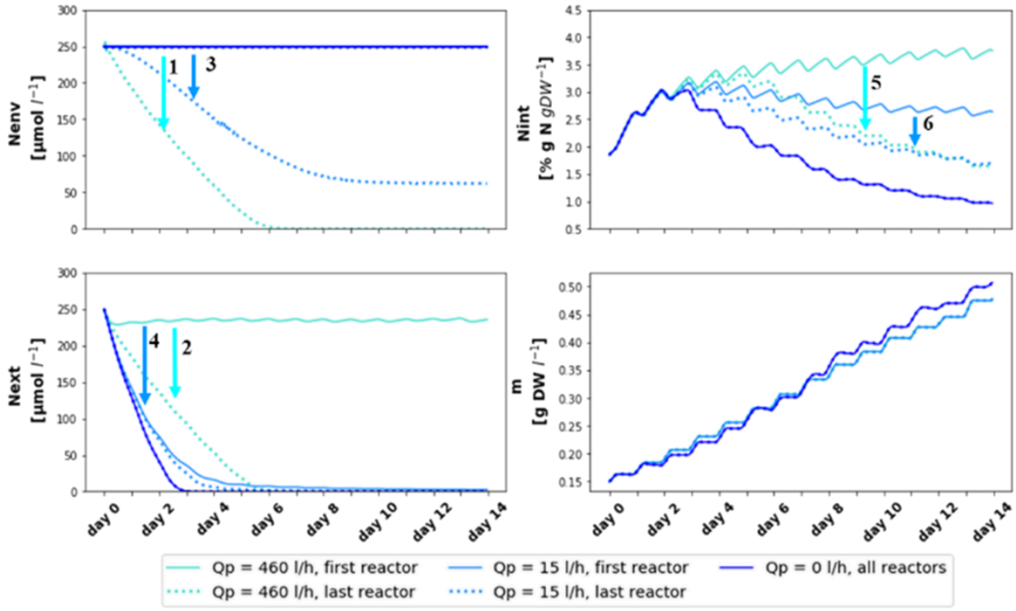

Fig. 5. N_{env}, N_{ext}, N_{int} and m dynamics along a 14 days cultivation period, simulating Q_p values of 0, 15 and 460 l·hour^{-1}. Arrows highlight differences between first and last reactor: N_{env} differences for Q_p=460 l·hour^{-1} (1) and for Q_p=15 l·hour^{-1} (3), N_{ext} differences for Q_p=460 l·hour^{-1} (2) and for Q_p=15 l·hour^{-1} (4) and N_{int} differences for Q_p=460 l·hour^{-1} (5) for Q_p=460 l·hour^{-1} (6). Simulation parameters and IC: 731 reactors, spring season, $N_{\mathrm{env}_0} = 250$ µM-N, $d = 0$.

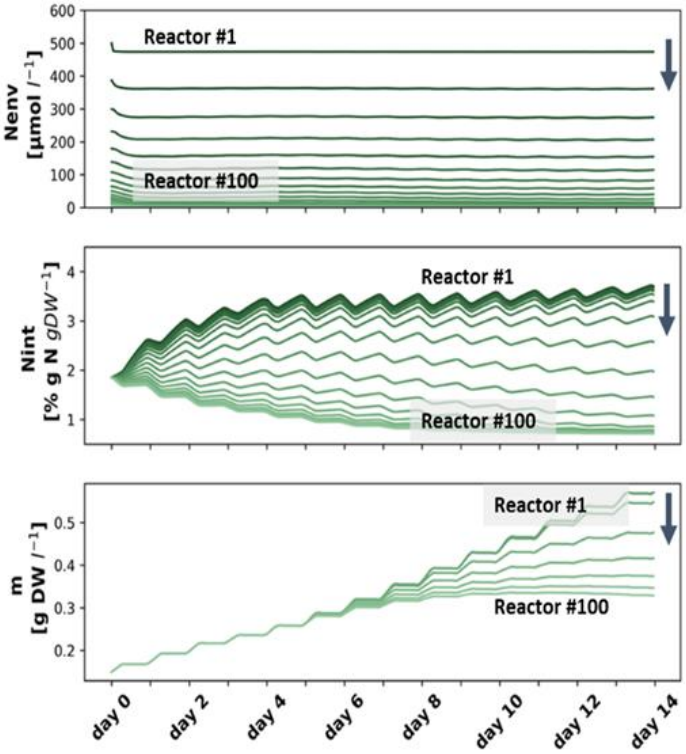

Fig. 6. N_{env}, N_{int} and m dynamics along a 14 days cultivation period in a diluting environment in a farm of 100 chained reactors. The lines represent N_{env}, N_{int} or m in each fifth reactor, starting from x=1 (darkest green) and progressing downstream along the arrows towards the last reactor (x=100, lightest green). Simulation parameters and IC: spring season, $N_{\mathrm{env}_0} = 500$ µM-N, $d = 0.05$.